5296 *Inorg. Chem.* **2009**, *48*, 5296–5302
DOI: 10.1021/ic900264x

Inorganic Chemistry
Article

High-Temperature Order−Disorder Transition in $CoCr_2Se_4$ and Trapping Co Disorder in Monoclinic $CoCr_2Se_4$: Structural Features of $Cu_{1-x}Co_xCr_2Se_4$ Phases

Volodymyr Svitlyk and Yurij Mozharivskyj*

Department of Chemistry, McMaster University, Hamilton, ON, Canada, L8S 4M1

Received February 10, 2009

X-ray diffraction studies on the $Cu_{1-x}Co_xCr_2Se_4$ system (x = 0, 0.2, 0.4, 0.6, 0.8, 1) proved the existence of the cubic spinel-type structure for $x \leq 0.2$ and the monoclinic Cr_3S_4-type one for $x \geq 0.8$. $CoCr_2Se_4$ undergoes an order−disorder phase transition above 750 °C. The high-temperature $CoCr_2Se_4$ polymorph crystallizes in the filled GdI_2-type structure with the $P\bar{3}m1$ space group. The trigonal-to-monoclinic symmetry breaking in $CoCr_2Se_4$ is found to be first-order within Landau theory. Co distribution in the low-temperature monoclinic $CoCr_2Se_4$ structure depends on cooling conditions of trigonal $CoCr_2Se_4$: rapid quenching results in Co disorder in the monoclinic structure, while slow cooling yields a fully ordered monoclinic structure.

1. Introduction

Coupling between ferromagnetic and structural transitions has been shown to yield good magnetocaloric properties.[1−3] While the conventional magnetocaloric effect has been known for more than a century,[4] it has never become an important cooling technique at or around room temperature because of its low efficiency. However, the 1997 discovery of the giant magnetocaloric effect in $Gd_5Si_2Ge_2$[1] and a successful test of a rotary magnetic refrigerator[5] suggested that magnetic refrigeration may become competitive, provided high-performance, environmentally friendly, and low-cost magnetocaloric materials are found. As shown for the $Gd_5(Si,Ge)_4$ alloys, the total isothermal entropy change doubles when the ferromagnetic ordering is coupled to a first-order structural transition. [6] Such intrinsic coupling between the magnetic and structural transitions is regarded to be a key element in achieving desired magnetocaloric properties.

Among intermetallic phases that exhibit ferromagnetic ordering at or above room temperature and offer a possibility of structural manipulation through a chemical substitution are the spinel phases of chromium with the general formula ACr_2X_4 (with A = Cd, Zn, Hg, Ga, Cu and X = O, S, Se, Te).[7] For $CuCr_2Se_4$, which orders ferromagnetically at 450 K,[8] it has been shown that a Co substitution on the Cu site introduces a first-order transition to monoclinic Cr_3S_4-type phases.[9] Monoclinic $CoCr_2Se_4$, the end member of the $Cu_{1-x}Co_xCr_2Se_4$ series, shows an antiferromagnetic ordering around 190 K.[10] However, the magnetic behavior of the $Cu_{1-x}Co_xCr_2Se_4$ phases with x varying between 0 and 1 has not been reported; additionally, the structure of monoclinic phases has never been verified using single-crystal diffraction techniques. As a part of our research on magnetically active materials, we undertook a systematic investigation of structural and magnetic features of the $Cu_{1-x}Co_xCr_2Se_4$ phases. Here, we present the structural part of our studies, which revealed interesting structural transformations for $CoCr_2Se_4$.

2. Experimental Section

2.1. Synthesis. Starting materials were powders of Cu (99.999%, CERAC Inc.), Co (99.8%, CERAC Inc.), Cr (99.95%, CERAC Inc.), and Se (99.99%, Alfa Aesar). Powders with the $Cu_{1-x}Co_xCr_2Se_4$ composition (x = 0, 0.2, 0.4, 0.6, 0.8, 1) and a total mass of 1 g were mixed and pressed in an Ar-filled drybox. All subsequent handling was also performed in the drybox. The pallets were sealed in evacuated silica tubes and treated at 800 °C for 50 h. After being quenched in cold water, the samples were reground, pressed, sealed in evacuated silica

*To whom correspondence should be addressed. E-mail: mozhar@mcmaster.ca.

(1) Pecharsky, V. K.; Gschneidner, K. A.Jr. *Phys. Rev. Lett.* **1997**, *78*, 4494–4497.
(2) Zhang, X. X.; Wen, G. H.; Wang, F. W.; Wang, W. H.; Yu, C. H. Wu, G. H. *Appl. Phys. Lett.* **2000**, *77*, 3072–3074.
(3) Tegus, O.; Brick, E.; Buschow, K. H. J.; de Boer, F. R. *Nature (London, U. K.)* **2002**, *415*, 150–152.
(4) Warburg, E. *Annal. Phys. Chem.* **1881**, *13*, 141.
(5) Zimm, C. B.; Sternberg, A.; Jastrab, A. G.; Boeder, A. M.; Lawton, L. M., Jr.; Chell, J. J. Rotating bed magnetic refrigeration apparatus. 6526759, 2003.
(6) Pecharsky, V. K.; Gschneidner, K. A.Jr. *Springer Ser. Mater. Sci.* **2005**, *79*, 199–222.
(7) Warczewski, J.; Krok-Kowalski, J. *J. Phys. Chem. Solids* **2003**, *64*, 1609–1614.
(8) Rodic, D.; Antic, B.; Tellgren, R.; Rundlof, H.; Blanusa, J. *J. Magn. Magn. Mater.* **1998**, *187*, 88–92.
(9) Smirnov, S. G.; Rozantsev, A. V.; Kesler, Y. A.; Gordeev, I. V.; Tret'yakov, Y. D. *Izv. Akad. Nauk SSSR, Neorg. Mater.* **1983**, *19*, 886–8.
(10) Morris, B. L.; Russo, P.; Wold, A. *J. Phys. Chem. Solids* **1970**, *31*, 635–8.

Published on Web 05/11/2009

Table 1. Lattice Constants for the Single-Phase Samples $CuCr_2Se_4$, $Cu_{0.8}Co_{0.2}Cr_2Se_4$, $Cu_{0.2}Co_{0.8}Cr_2Se_4$, and $CoCr_2Se_4$ from Powder Diffraction Data

sample	space group	*a*, Å	*b*, Å	*c*, Å
$CuCr_2Se_4$	$F4\bar{3}m$	10.3258(1)		
$Cu_{0.8}Co_{0.2}Cr_2Se_4$	$F4\bar{3}m$	10.32257(7)		
$Cu_{0.2}Co_{0.8}Cr_2Se_4$	$C2/m$	13.0758(9)	3.6075(2), β = 117.875(4)°	6.2348(5)
$CoCr_2Se_4$	$C2/m$	13.0163(9)	3.6100(3), β = 117.904(5)°	6.2497(5)

Table 2. Crystal Data and Structure Refinements for $Cu_{0.8}Co_{0.2}Cr_2Se_4$ and $CoCr_2Se_4$ at 20 °C, Using Mo Kα Radiation and a STOE IPDS II Diffractometer

sample	$Cu_{0.8}Co_{0.2}Cr_2Se_4$	$CoCr_2Se_4$ (quenched)	$CoCr_2Se_4$ (slowly cooled)
space group	$F4\bar{3}m$	$C2/m$	$C2/m$
lattice parameters, Å	a = 10.331(3)	a = 13.089(5) b = 3.592(2) c = 6.223(2) β = 118.66(3)°	a = 13.025(6) b = 3.606(1), c = 6.263(3) β = 117.88(3)°
volume, Å^3	1102.6(6)	256.7(2)	260.0(2)
Z	8	2	2
density (calcd), g/cm^3	5.813	6.194	6.115
cryst size, mm^3	0.024 × 0.052 × 0.080	0.037 × 0.057 × 0.098	0.011 × 0.025 × 0.037
2θ range	6.84−58.22°	7.10−57.76°	7.08−58.34°
index ranges	$-13 \le h \le 13$, $-12 \le k \le 13$, $-13 \le l \le 13$	$-14 \le h \le 17$, $-4 \le k \le 4$, $-8 \le l \le 8$	$-17 \le h \le 17$, $-4 \le k \le 4$, $-8 \le l \le 6$
reflns collected	2398	1227	699
independent reflns	88 [R_{int} = 0.131]	391 [R_{int} = 0.069]	385 [R_{int} = 0.075]
completeness to 2θ	93.6%	99.7%	95.3%
data/restraints/par.	88/0/8	391/0/25	365/0/25
goodness-of-fit on F^2	1.183	1.149	0.846
final R indices [$I > 2\sigma(I)$]	R_1 = 0.050, wR_2 = 0.084	R_1 = 0.072, wR_2 = 0.206	R_1 = 0.055, wR_2 = 0.083
R indices (all data)	R_1 = 0.069, wR_2 = 0.089	R_1 = 0.092, wR_2 = 0.221	R_1 = 0.138, wR_2 = 0.100
extinction coefficient	0.0002(1)	0.008(4)	0
diff. peak/ hole, e/Å^3	1.634 /-0.760	2.891/−2.592	2.475/−1.649

Table 3. Atomic and Isotropic Temperature (U) Parameters for $Cu_{0.8}Co_{0.2}Cr_2Se_4$ and $CoCr_2Se_4$ from Single-Crystal Diffraction Data

atom		occupancy	*x*/*a*	*y*/*b*	*z*/*c*	*U* (Å^2)
			$Cu_{0.8}Co_{0.2}Cr_2Se_4$			
Cu	8*a*	0.80[a]	5/8	5/8	5/8	0.020(1)
Co	8*a*	0.20[a]	5/8	5/8	5/8	0.020(1)
Cr	16*d*	1	0	0	0	0.019(1)
Se	32*e*	1	0.2424(1)	0.2424(1)	0.2424(1)	0.020(1)
			$CoCr_2Se_4$ (quenched)			
Co1	2*a*	0.77(1)	0	0	0	0.049(2)
Co2	2*d*	0.23(1)	0	1/2	1/2	0.049(2)
Cr	4*i*	1	0.2540(3)	0	0.2677(5)	0.031(1)
Se1	4*i*	1	0.3694(2)	0	0.0348(3)	0.0276(9)
Se2	4*i*	1	0.1215(2)	0	0.4537(2)	0.0284(9)
			$CoCr_2Se_4$ (slowly cooled)			
Co	2*a*	0.95(2)[b]	0	0	0	0.011(2)
Cr	4*i*	1	0.2567(4)	0	0.2774(10)	0.0112(9)
Se1	4*i*	1	0.3674(2)	0	0.0296(6)	0.0102(8)
Se2	4*i*	1	0.1182(2)	0	0.4512(6)	0.0098(8)

[a] Occupancy is not refined. [b] The occupancy is assumed to be 1 in the $CoCr_2Se_4$ formula.

tubes, and annealed at 800 °C for 2 weeks, followed by quenching in cold water. After this treatment, the $CoCr_2Se_4$ sample was again heated to 800 °C, annealed for 4 h, and cooled at the rate of 15 °C/h to room temperature.

2.2. X-Ray Analysis. Room-temperature X-ray powder diffraction patterns in the 20−90° 2θ range were recorded on a PANalytical X'Pert Pro diffractometer with an X'Celerator detector and Cu $K_{\alpha 1}$ radiation. The full-profile Rietveld refinement (Rietica program[11]) was used for phase analyses, to derive lattice constants and refine atomic parameters (Table 1 and Supporting Information). High-temperature (HT) X-ray powder diffraction patterns for $CoCr_2Se_4$ in the 20−90° 2θ range were collected on the PANalytical X'Pert Pro diffractometer with an X'Celerator detector but with Cu K_α radiation for faster data collection and better intensity statistics. The data were recorded at 25 °C and in the 50−800 °C region with a 50 °C step in the Anton Paar HTK 2000 high-temperature chamber with flowing He and 5 vol % CO and a Pt sample heater.

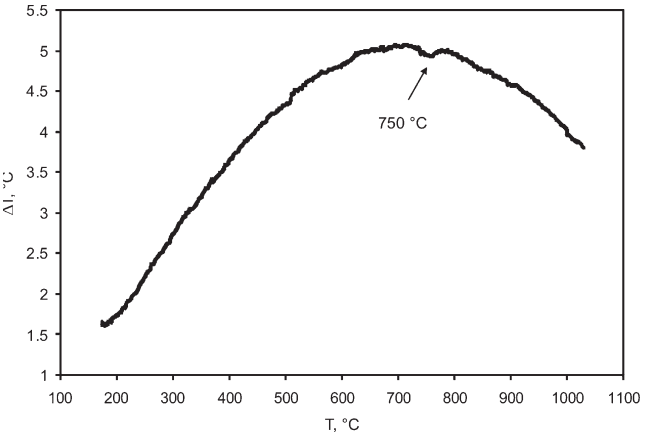

Figure 1. Differential thermal analysis for the quenched $CoCr_2Se_4$ sample.

Single-crystal X-ray diffraction data for crystals extracted from the quenched $Cu_{0.8}Co_{0.2}Cr_2Se_4$ and $CoCr_2Se_4$ samples and slowly cooled $CoCr_2Se_4$ sample were collected on a STOE IPDSII diffractometer with Mo Kα radiation. A numerical absorption correction was based on the crystal shape that was originally derived from the optical face indexing but later optimized against equivalent reflections using the STOE X-Shape software.[12] Structural refinements were performed

(11) Hunter, B. A.; Howard, C. J. *Rietica*; Australian Nuclear Science and Technology Organization: Menai, Austalia, 2000.

(12) *X-SHAPE*, version 2.05; *X-RED32*, version 1.10, STOE & Cie GmbH: Darmstadt, Germany, 2004.

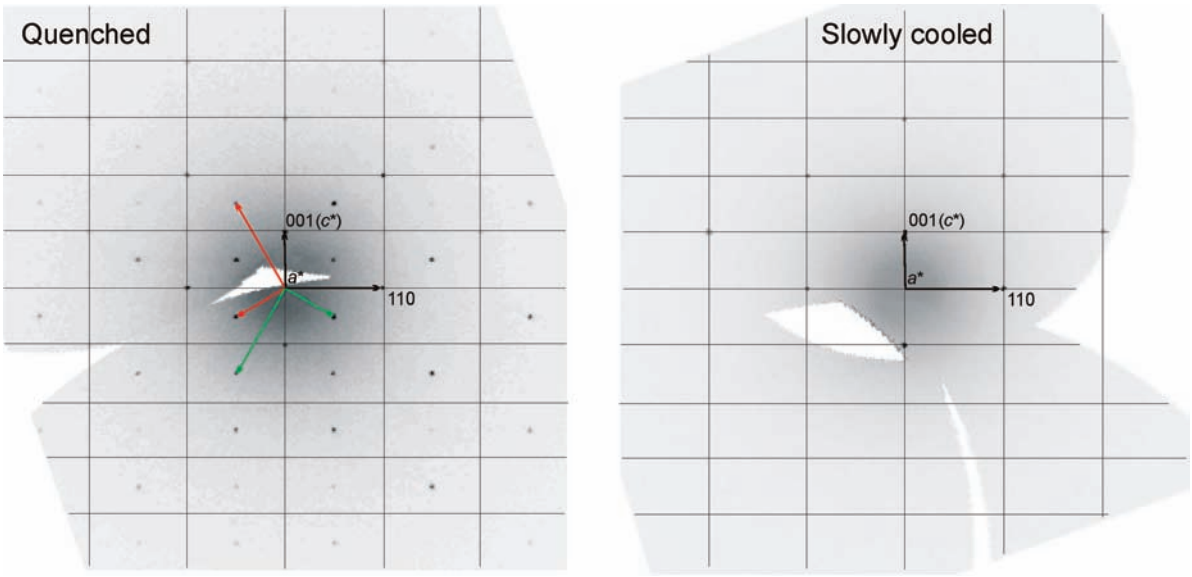

Figure 2. Reciprocal layer normal to a^* for the quenched (right) and slowly cooled (left) monoclinic $CoCr_2Se_4$ crystals. Lattice translations corresponding to the three twinned components are shown by different colors. The grid lines outline the lattice of one twin component, chosen as a primary one.

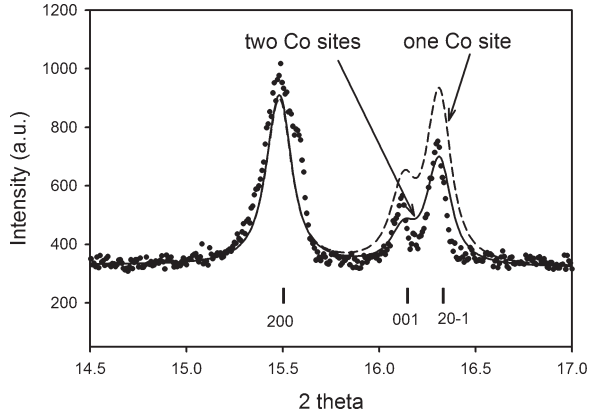

Figure 3. Rietveld fits of the X-ray powder data for the quenched monoclinic $CoCr_2Se_4$ phase using two structural models (see text). Only a small 2Θ region is shown.

using the SHELXL program (Tables 2 and 3).[13] Further details of the crystal structure investigations can be obtained from the Fachinformationszentrum Karlsruhe, 76344 Eggenstein-Leopoldshafen, Germany (fax: (49) 7247−808−666; e-mail: crysdata@fiz-karlsruhe.de), on quoting the depository CSD numbers 420367 for quenched $Cu_{0.2}Co_{0.8}Cr_2Se_4$, 420365 for quenched $CoCr_2Se_4$, and 420366 for slowly cooled $CoCr_2Se_4$, and these are also available in the Supporting Information.

2.3. Thermal Analysis. Differential thermal analysis (DTA) for the quenched $CoCr_2Se_4$ sample was performed on a Netzsch STA-409 apparatus in the 175−1030 °C temperature range with an average 2.5 °C step and 10 °C/min heating rate (Figure 1). The vertical axis on the graph corresponds to the temperature difference between the sample and reference thermocouples, and its values are proportional to the heat flow.

3. Results and Discussion

3.1. Homogeneity Regions and Structures of the $Cu_{1-x}Co_xCr_2Se_4$ Phases. Phase analysis of the $Cu_{1-x}Co_xCr_2Se_4$ series indicated that the cubic spinel structure exists at least to $x = 0.2$, while the monoclinic Cr_3S_4-type structure appears at most at $x = 0.8$. Samples with $x = 0.4$ and 0.6 were found to be mixtures of both cubic and monoclinic phases. Cell dimensions for the single-phase samples are given in Table 1. The homogeneity ranges established by us for $Cu_{1-x}Co_xCr_2Se_4$ agree well with the results of Smirnov et al.[9] but deviate somewhat from the data of Maciazek et al.[14]

Structures of two members, cubic $Cu_{0.8}Co_{0.2}Cr_2Se_4$ and monoclinic $CoCr_2Se_4$, were verified through single-crystal and powder X-ray diffraction. Analysis of the diffraction spots from the single crystal of $Cu_{0.8}Co_{0.2}Cr_2Se_4$ at room temperature revealed no unusual features, and the refinement with the initial atomic parameters taken from $CuCr_2Se_4$[15] converged well (Tables 2 and 3). Due to the similar scattering powers of Cu and Co, the occupancy of the 8*a* site was fixed at 80% of Cu and 20% of Co during the refinement. Structural features of $CoCr_2Se_4$ were found to depend strongly on the cooling conditions, and this is discussed below.

3.2. HT Order−Disorder Transition in $CoCr_2Se_4$: Quenching Co Disorder in the Monoclinic Structure. Diffraction spots of the single crystal extracted from the quenched $CoCr_2Se_4$ sample could be indexed to three pseudomerahedral monoclinic twin lattices rotated around the a^* direction by 120° (Figure 2). The structural refinement against the data integrated for one component led to the deficient Co site (~77% occupancy) and a significant additional electron density of 7.97 e/A^3 at $x = 0$, $y = 1/2$, and $z = 1/2$. Assigning this extra electron density to "missing" Co atoms and confining the total occupancy of the two Co sites to 1 improved the refinement and yielded smoother residual electron density. Introducing three twin components into the refinement either through a matrix transformation in the control file (the *hkl*4 data set) or through the intensity integration

(13) Sheldrick, G. M. *SHELXL97*; *SHELXS97*; University of Gottingen: Gottingen, Germany, 1997.

(14) Maciazek, E.; Molak, A.; Goryczka, T. *J. Alloys Compd.* **2007**, *441*, 222–230.

(15) Okonska-Kozlowska, I.; Kopyczok, J.; Lutz, H. D.; Stingl, T. *Acta Crystallogr., Sect. C* **1993**, *C49*, 1448–9.

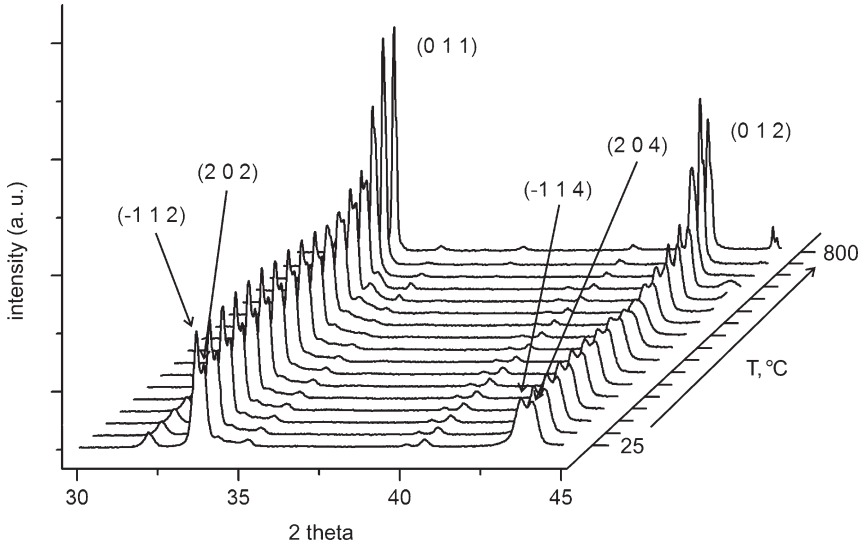

Figure 4. Temperature-dependent X-ray powder diffraction scans for the quenched $CoCr_2Se_4$ sample.

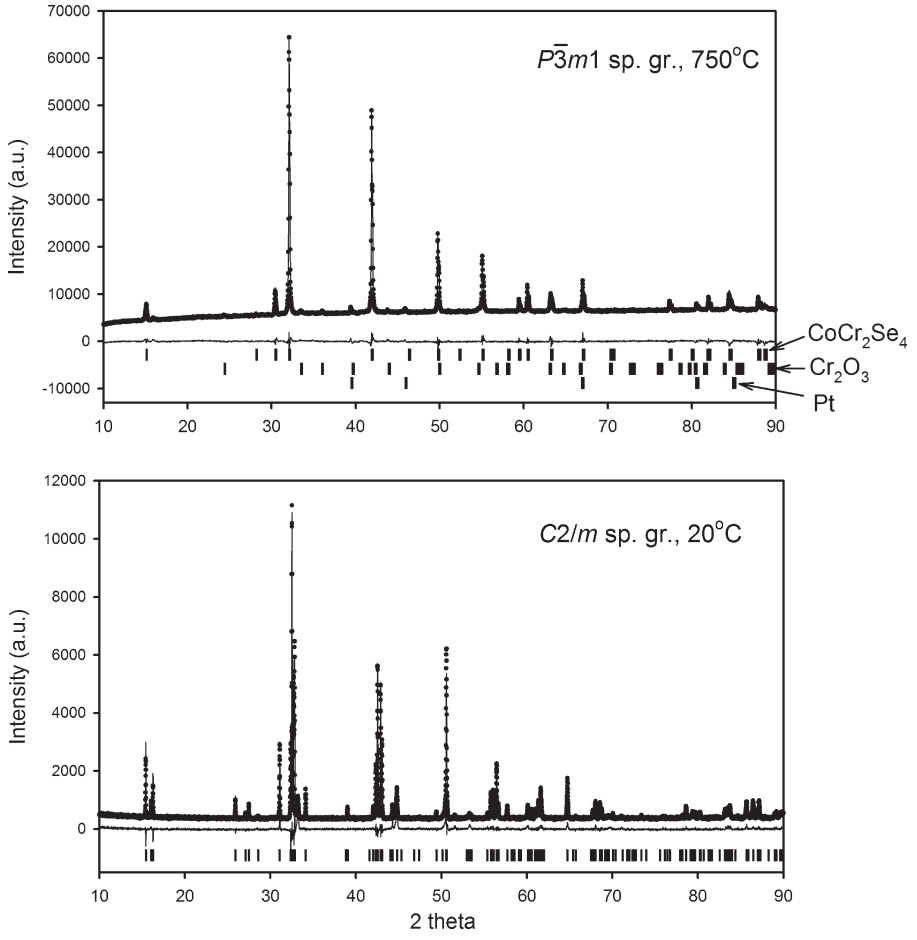

Figure 5. Rietveld refinements of the X-ray powder data for $CoCr_2Se_4$ at 750 and 20 °C. Data at 20 °C are for the slowly cooled $CoCr_2Se_4$ sample.

with three twin components (the *hkl*5 data set) did not eliminate the electron density at $x = 0$, $y = 1/2$, and $z = 1/2$. The presence of the two Co sites was verified through X-ray powder diffraction, which is immune to twinning problems. The model with two deficient Co positions yielded a better profile fit and lower agreement factors than the model with one fully occupied Co site ($R_p = 0.068$ and $R_I = 0.052$ versus $R_p = 0.073$ and $R_I = 0.060$). In powder diffraction, the difference between the two models manifests itself distinctly in the intensity ratio between three peaks around $2\theta = \sim 16°$ (Figure 3). The occupancies of the Co1 and Co2 sites refined from powder data were 84.8(5)% and 15.2(5)%.

The pseudomerahedral twinning observed for the monoclinic $CoCr_2Se_4$ crystal could have resulted from a trigonal-to-monoclinic symmetry breaking upon

Table 4. Powder Refinement Data for $CoCr_2Se_4$ at 750 °C

Space group	$P\bar{3}m1$
lattice parameters, Å	a = 3.66434(5)
	c = 5.88253(8)
volume, Å^3	68.405(2)
Z	0.5
radiation	Cu$K\alpha$
2θ range	10−90°
data collection step	0.0167°
N_{hkl}	33
atomic params refined	5
R_p	0.017
R_{wp}	0.025
R_I	0.013

[a] $R_I = \sum|I_o - I_c|/\sum|I_o|$, $R_p = \sum|y_{oi} - y_{ci}|/\sum|y_{oi}|$, $R_{wp} = (\sum w_i(y_{oi} - y_{ci})^2/\sum w_i(y_{oi})^2)^{1/2}$, $w_i = (y_{oi})^{-1/2}$.

Table 5. Atomic and Isotropic Temperature (B) Parameters for Trigonal $CoCr_2Se_4$ from Powder Diffraction Data at 750 °C

atom		occupancy	x/a	y/b	z/c	B (Å^2)
Co	1a	0.54(1)	0	0	0	0.7(3)
Cr	1b	1	0	0	1/2	1.5(2)
Se	2d	1	1/3	2/3	0.2509(2)	1.3(1)

quenching from 800 °C to room temperature. This hypothesis gained some ground when an endothermic peak around 750 °C was observed during the DTA analysis for the $CoCr_2Se_4$ powder (Figure 1). The subsequent HT powder diffraction proved that the monoclinic structure does transform into a higher-symmetry structure at 750 °C (Figure 4). In order to derive a high-symmetry space group, the transition was treated as a second-order one (in reality, it is first-order, as discussed below). According to the Landau theory of second-order phase transitions, the following trigonal space groups, $P\bar{3}1m$, $P\bar{3}m1$, and $R\bar{3}m$, could yield the $C2/m$ space group. Without increasing the number of independent sites in a high-symmetry unit cell, the atomic arrangement of the $C2/m$ unit cell could be derived only from the unit cell with $P\bar{3}m1$ symmetry and with Co being at $x = 0$, $y = 0$, and $z = 0$; Cr at 0, 0, and 1/2; and Se at 1/3, 2/3, and ∼0.25. The two deficient Co sites of the monoclinic cell were merged into one deficient site (occupancy 50%) in the trigonal cell. This HT structural model was verified by the full profile Rietveld refinement, which yielded an excellent fit between the experimental and calculated powder patterns at 750 °C (Figure 5, Tables 4 and 5). The occupancy of the Co site was refined to 54(1)%, which comes close to the assumed 50%.

The $C2/m$-to-$P\bar{3}m1$ transition found by us for $CoCr_2Se_4$ at high temperatures was also observed for other phases that adopt a monoclinic Cr_3S_4-type structure at room temperature, for example, $Cr_{3\pm x}Se_4$,[16] $Cr_xTi_2Se_4$,[17] and $Fe_xV_2S_4$.[18] The $P\bar{3}m1$ structure with the atomic arrangement of HT $CoCr_2Se_4$ is referred to most commonly as CdI_2.[16,19] This classification is rather unfortunate, as there are no metal atoms between alternative layers of iodine atoms in GdI_2, while there are such in HT $CoCr_2Se_4$ and related phases. If the CdI_2 structure were to be retained for the description of HT $CoCr_2Se_4$ and related phases, then we should emphasize that the structure of interest is a filled version of the CdI_2 structure. The literature search revealed that similar atomic arrangements are also known as the $Cr_{0.88}S$, [20] $CdTlS_2$, [21] $ZrFe_{0.16}Se_2$,[22] and $NiCuSb_2$[23] structures. In some cases, such as in $NiCr_2S_4$,[19] the monoclinic form transforms into the HT-deficient NiAs structure ($P6_3/mmc$ space group), in which both metals are statistically distributed on one site with a total occupancy of 75%. The powder patterns of the two structures can be easily distinguished by the 001 peak around $\sim 2\theta = 15°$. Due to the extinction conditions, such a peak should be absent in the $P6_3/mmc$ space group (NiAs structure) but is allowed in the $P\bar{3}m1$ space group (filled CdI_2 structure).

When the $CoCr_2Se_4$ sample annealed at 800 °C is slowly cooled to room temperature, the diffraction spots from the extracted single crystal could be indexed only to one monoclinic cell (Figure 2). The single-crystal refinement yielded full occupancy within three standard deviations for the Co site (95(2)%), and no significant electron density was observed at $x = 0$, $y = 1/2$, and $z = 1/2$. These results were in good agreement with those obtained from the full profile Rietveld powder refinement for the slowly cooled sample (Figure 5 and the Supporting Information). It has to be pointed out that the powder diffraction profile of the slowly cooled sample had much narrower, better-defined diffraction peaks than the quenched sample (see Figure 6). Such a difference suggests that, during quenching, a long-range order is not fully established in the monoclinic structure.

In view of our single-crystal and powder diffraction results, we can state that the high-temperature form of $CoCr_2Se_4$ adopts a trigonal unit cell, in which Co atoms are statistically distributed in octahedra between the Se layers. On average, only half of those octahedra are being populated by Co atoms. Upon slow cooling, the Co atoms tend to order in alternative fashion in the layer and between the layers, and the monoclinic lattice results. However, rapid quenching does not allow all Co atoms to order completely, and two deficient sites are formed (Figure 6). To our knowledge, it is the first time that the possibility of quenching the disorder has been explicitly shown for the Cr_3S_4-type phases and has been related to the cooling conditions.

3.3. Nature of the Symmetry Breaking in $CoCr_2Se_4$. Transitions between different crystal modifications can take place via abrupt, *first-order* reconstruction of the crystal lattice (e.g., Mn_5Si_3-type (LT) ↔ Yb_5Sb_3-type (HT) transformation in Gd_5Bi_3 [24]) or gradual, *second-order* changes in the atomic arrangement (e.g., $P4/nmm$ to $Pmmn$ transitions in $RECuAs_{2-x}P_x$ with RE = Sm, Gd, Ho, Er [25−28]).

(16) Ohtani, T.; Fujimoto, R.; Yoshinaga, H.; Nakahira, M.; Ueda, Y. *J. Solid State Chem.* **1983**, *48*, 161–7.
(17) Ohtsuka, N.; Kosuge, K.; Nakayama, N.; Ueda, Y.; Kachi, S. *J. Solid State Chem.* **1982**, *45*, 411–12.
(18) Oka, Y.; Kosuge, K.; Kachi, S. *Mater. Res. Bull.* **1980**, *15*, 521–4.
(19) Vaqueiro, P.; Hull, S.; Lebech, B.; Powell, A. V. *J. Mater. Chem.* **1999**, *9*, 2859–2863.
(20) Jellinek, F. *Acta Crystallogr.* **1957**, *10*, 620–8.
(21) Avilov, A. S.; Agaev, K. A.; Guseinov, G. G.; Imamov, R. M. *Kristallografiya* **1969**, *14*, 443–6.
(22) Gleizes, A.; Revelli, J.; Ibers, J. A. *J. Solid State Chem.* **1976**, *17*, 363–72.
(23) Kabalov, Y. K.; Sokolova, E. V.; Spiridonov, E. M.; Spiridonov, F. M. *Dokl. Akad. Nauk* **1994**, *335*, 709–11.
(24) Svitlyk, V.; Fei, F.; Mozharivskyj, Y. *J. Solid State Chem.* **2008**, *181*, 1080–1086.
(25) Mozharivskyj, Y.; Kaczorowski, D.; Franzen, H. F. *J. Solid State Chem.* **2000**, *155*, 259–272.

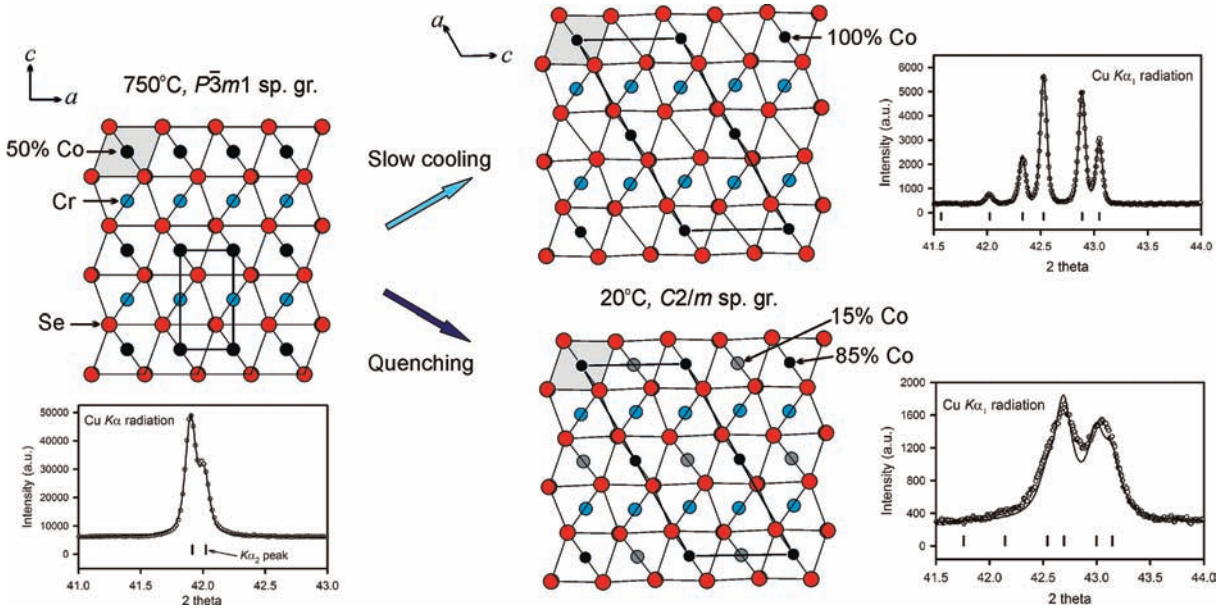

Figure 6. Development of the monoclinic $CoCr_2Se_4$ structures from the high-temperature trigonal one during slow cooling and quenching. The powder patterns on the right represent peak splitting due to the reduction of symmetry as well as peak broadening (quenched sample) associated with the short-range order.

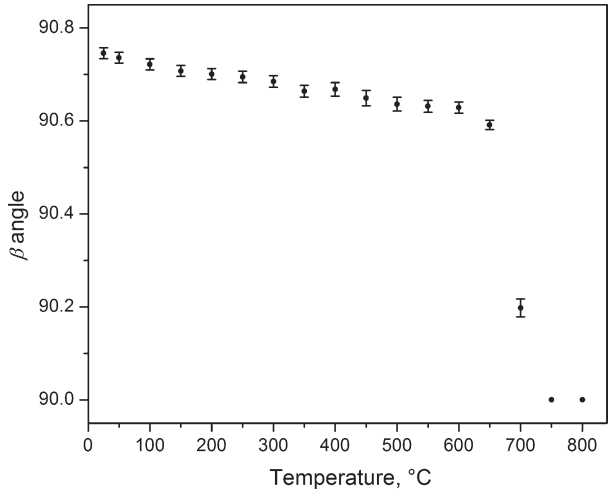

Figure 7. Change in the monoclinic β angle with the temperature.

A question of whether a transition between the high- and low-symmetry structures can occur as second-order (continuous) is analyzed within the framework of Landau theory using group-theoretical considerations.[29,30] One of the conclusions of Landau theory is that two phases cannot coexist during a second-order transition, while they can during a first-order one.[31] While the HT powder diffraction data (Figure 4) do not show coexistence of the two $CoCr_2Se_4$ modifications and, together with the monoclinic β angle (Figure 7), point rather to a gradual symmetry change, the transition can still occur via small but abrupt changes and, thus, be first-order in nature.

The first consideration of Landau theory is to establish a wave vector, **k**, corresponding to the symmetry breaking in the sense that any lost translation (vectors $\mathbf{T}_i$) yields nonintegral values for $\mathbf{k}\cdot\mathbf{T}_i/2\pi$.[32] Since the unit cell is doubled along a_{trig} and c_{trig} (or simply a and c) of the trigonal cell ($P\bar{3}m1$), the **k** vector of the distortion is $\mathbf{k} = 1/2\mathbf{a}^* + 1/2\mathbf{c}^*$. The second step is to find a group of the wave vector. The wave vector transforms into itself (or the + modulo of a reciprocal lattice vector) under E, C_{2x}, i, and σ_x, and the order, $g_o(\mathbf{k})$, of this point group, $\mathcal{L}_o(\mathbf{k})$, is 4. Since the ratio between the order, g_o, of the point group of the high-symmetry space group and the order, $g_o(\mathbf{k})$, of the point group of the wave vector is 3 ($g_o/g_o(\mathbf{k}) = 12/4 = 3$), third-order invariants will exist in the expansion of the Gibbs free energy, and thus, the distortion with $\mathbf{k} = 1/2\mathbf{a} + 1/2\mathbf{c}$ will be first-order in nature.[31] While the first two rules of Landau theory, namely, that the high-symmetry and low-symmetry space groups are in a group−subgroup relationship and that the transition corresponds to a single irreducible representation, are obeyed, the presence of third-order invariants will lead to a coexistence of the two phases at the transition point and, thus, to an abrupt atomic rearrangement.

The $P\bar{3}m1 \rightarrow C2/m$ symmetry breaking can proceed along three equivalent directions in the *ab* plane of the trigonal lattice, corresponding to the three 2-fold axes: namely, along a ($\mathbf{k} = 1/2\mathbf{a}^* + 1/2\mathbf{c}^*$), b ($\mathbf{k} = 1/2\mathbf{b}^* + 1/2\mathbf{c}^*$), and $a + b$ ($\mathbf{k} = 1/2\mathbf{a}^* + 1/2\mathbf{b}^* + 1/2\mathbf{c}^*$). Thus, three monoclinic domains rotated around c_{trig} by 120° will be formed (Figure 8), and twinning can be expected for a rapidly cooled sample. Such coexistence of twin components will manifest itself in pseudomerohedral twinning,

(26) Mozharivskyj, Y.; Kaczorowski, D.; Franzen, H. F. *Z. Anorg. Allg. Chem.* **2001**, *627*, 2163–2172.
(27) Mozharivskyj, Y.; Franzen, H. F. *J. Phys. Chem. B* **2002**, *106*, 9528–9535.
(28) Mozharivskyj, Y.; Pecharsky, A. O.; Bud'ko, S.; Franzen, H. F. *Z. Anorg. Allg. Chem.* **2002**, *628*, 1619–1630.
(29) Franzen, H. F. *Chem. Mater.* **1990**, *2*, 486–91.
(30) Landau, L. D.; Lifshitz, E. M. *Statistical Physics*; Pergamon Press: London, 1958; Vol. *5*, p 515.
(31) Landau, L. D.; Lifshitz, E. M. In *Statistical Physics*; Pergamon Press: London, 1958; Vol. *5*, p 445.
(32) Franzen, H. F. *Physical Chemistry of Solids*; World Scientific: Singapore, 1994; p 296.

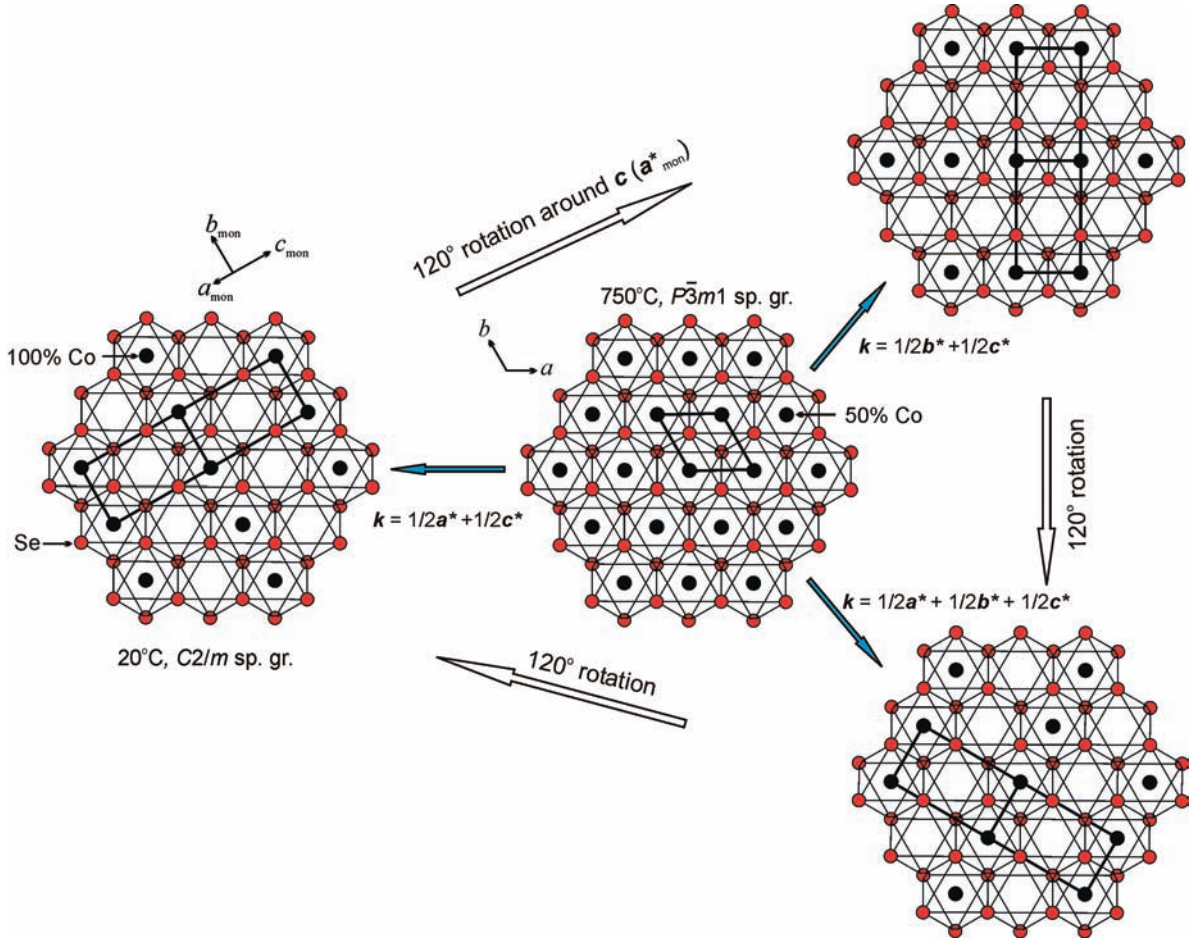

Figure 8. Formation of three twin components corresponding to the three **k** vectors. Only one $_{\infty}^{2}$[$CoSe_4$] layer is shown. Co atoms are inside the Se octahedra.

as observed during the single-crystal diffraction. However, if the sample is slowly cooled, one twin component may grow by consuming the other components, and the twinning may disappear.

The $P\bar{3}m1 \rightarrow C2/m$ distortion involves both displacive and order−disorder atomic rearrangements. For monoclinic $CoCr_2Se_4$, the atomic displacements defined as shifts from the ideal positions in the trigonal lattice are very small. Therefore, the trigonal lattice is unlikely to be quenched, as the energy barrier to the monoclinic lattice is small and can be overcome by the enthalpy contribution to the Gibbs free energy. On the other hand, atomic ordering during $P\bar{3}m1 \rightarrow C2/m$ involves moving Co atoms from one Se octahedron into another so that the alternative rows of Se octahedra become empty in the $_{\infty}^{2}$[$CoSe_4$] layer (Figure 8) and also along the c_{trig} direction (Figure 6). Since the Se octahedra share edges within the $_{\infty}^{2}$[$CoSe_4$] layers, Co rearrangement is likely to be energy-demanding and can be suppressed by rapid quenching. These conclusions are supported by single-crystal and powder diffraction results for the quenched $CoCr_2Se_4$ sample, which revealed trapping of the Co disorder in the monoclinic structure.

4. Conclusions

On the basis of the pseudomerohedral twinning observed for the quenched single crystals, a high-temperature trigonal structure was predicted for $CoCr_2Se_4$ and confirmed by means of DTA and HT powder diffraction. The $P\bar{3}m1 \rightarrow C2/m$ symmetry breaking in $CoCr_2Se_4$ is found to be first-order in nature since the third-order invariants exist in the expansion of the Gibbs free energy describing the distortion pathway. For the first time, the feasibility of quenching the HT disorder in the LT Cr_3S_4-type phases has been clearly demonstrated.

Acknowledgment. This work was supported by a Discovery Grant from the Natural Sciences and Engineering Research Council of Canada.

Supporting Information Available: Additional tables and crystollographic information. This material is available free of charge via the Internet at http://pubs.acs.org.